Journal of Cleaner Production xxx (2016) 1–15

Contents lists available at ScienceDirect

Journal of Cleaner Production

journal homepage: www.elsevier.com/locate/jclepro

A normal boundary intersection with multivariate mean square error approach for dry end milling process optimization of the AISI 1045 steel

Danielle Martins Duarte Costa [a], Tarcísio Gonçalves Brito [a], Anderson Paulo de Paiva [a], Rafael Coradi Leme [b], Pedro Paulo Balestrassi [a, *]

[a] Institute of Industrial Engineering and Management, Federal University of Itajuba, Av. BPS, 1303, Itajuba, Minas Gerais 37500-188, Brazil
[b] Department of Industrial and Systems Engineering, University of Tennessee, Knoxville, 520 John D. Tickle Building, 851 Neyland Drive, Knoxville, TN 37996-2315, USA

ARTICLE INFO

Article history:
Received 3 July 2015
Received in revised form
11 December 2015
Accepted 23 January 2016
Available online xxx

Keywords:
Dry end milling
Optimization
Multivariate mean square error
Normal boundary intersection
Weighted sums

ABSTRACT

This research explores a new methodology to optimize a multivariate dry end milling process of the AISI 1045 steel. Once the use of cutting fluids in machining processes has been questioned, dry milling techniques are considered to be a way to the cleaner manufacturing in the context of the sustainable production. Four input parameters and six response variables were considered. The normal boundary intersection (NBI) is a multi-objective optimization method mainly developed to compensate the short comings attributed to the method of weighted sums. However, the NBI method tends to fail producing unreal results and non-convex frontiers if the multiple objective functions are correlated and with conflicting objectives. To deal with this constraint, this work presents a new multi-objective hybrid approach, called NBI-MMSE, that combine the NBI with multivariate mean square error (MMSE) functions. This approach utilizes a procedure that integrates the principal component analysis with the response surface methodology for problems with correlated multiple responses. Theoretical and experimental results indicate that the solution found by NBI-MMSE approach was characterized as a more appropriate optimal point in relation to one obtained with the traditional weighted sum. In this case, the process parameters optimization for end milling process without cutting fluids was able to achieve, at the same time, the maximum rate of removed material and minimum surface roughness, confirming the adequacy of the work's proposal.

© 2016 Elsevier Ltd. All rights reserved.

1. Introduction

Beside of the productivity and quality goals, the application of the concept of sustainability has become an important topic in machining processes. According to Fratila and Caizar (2011) the concept of sustainability and cleaner production can be understood to the creation of products and services that consider environment-friendly processes, that it be economically viable and healthful for employees. Concerning the application of the sustainability principles, considerable attention has been given to reduce or completely omit the cutting fluids during the machining processes (Fratila and Caizar, 2011; Jozić et al., 2015; Zhang et al., 2012).

The cutting fluids present some mechanisms for causing illness or injury in machine operators, including skin disorders and respiratory diseases. Furthermore, after their disposal and if the recycling is not possible, they may become polluting agents in soil and water when inappropriately handled. Cutting fluids also has influence on the costs of metal cutting industry (Fratila and Caizar, 2011; Ginting and Nouari, 2007; Jiang et al., 2015; Jozić et al., 2015; Zhang et al., 2012). By the other hand, the absence of fluids in metal cutting can become serious problems for machinability (surface finish and tool life) (Ginting and Nouari, 2007). Thus, a way to ensure dry machining can successfully be done in metal cutting is to provide the suitable cutting parameters.

In this respect, the concern to act on at the same time on quality, productivity and sustainable production have forced organizations

* Corresponding author. Tel.: +55 35 98877 6958; fax: +55 35 3629 1148.
E-mail addresses: danielle.costa@ifsuldeminas.edu.br (D.M. Duarte Costa), engtarc.gb@ig.com.br (T.G. Brito), andersonppaiva@unifei.edu.br (A.P. de Paiva), leme@unifei.edu.br (R.C. Leme), pedro@unifei.edu.br (P.P. Balestrassi).

http://dx.doi.org/10.1016/j.jclepro.2016.01.062
0959-6526/© 2016 Elsevier Ltd. All rights reserved.

Please cite this article in press as: Duarte Costa, D.M., et al., A normal boundary intersection with multivariate mean square error approach for dry end milling process optimization of the AISI 1045 steel, Journal of Cleaner Production (2016), http://dx.doi.org/10.1016/j.jclepro.2016.01.062

ARTICLE IN PRESS

Nomenclature

Adj-R^2	Adjusted R-squared
a_e	Radial depth of cut (mm)
a_p	Axial depth of cut (mm)
DC_{ap}	Cutting diameter at cutting depth, of the tool
f_z	Feed per tooth (mm/tooth)
k	Number of cutting parameters
MRR	Material removal rate (cm^3/min)
MSE	Mean square error method
N	Spindle speed (RPM)
NBI-MMSE	Normal boundary intersection with multivariate mean square error approach
PC	Principal component
PC_1	First principal component
PC_2	Second principal component
PC-scores	Principal components scores
P_{max}	Maximum phosphorus
R_a	Average surface roughness (μm)
R_q	Root mean square roughness (μm)
R_t	Maximum peak to valley (μm)
R_y	Maximum surface roughness (μm)
R_z	Ten point height roughness (μm)
S_{max}	Maximum sulfur
T	Tool life
VB_{max}	Maximum tool flank wear
V_c	Cutting speed (m/min)
WS-MMSE	Weighted sum with multivariate mean square error approach
Z	Number of effective teeth of the tool
α	Axial distance
$\beta_0,\beta_i,\beta_{ii},\beta_{ij}$	Coefficients
ρ	Design radius
λ_{PC}	Eigenvalue of the principal component
e_{ij}	Eigenvector of the principal component
μ_{Y_j}	Mean of the original response
$MMSE_i$, $MMSE_1$, $MMSE_2$	Multivariate mean square error functions
V_f	Table feed (mm/min)
$f_i(x_i^*)$	Nadir point
f^N	Nadir point
$\bar{f}_i(\mathbf{x})$, $\bar{f}_1(\mathbf{x})$, $\bar{f}_2(\mathbf{x})$	Normalized objective functions
$f_i(x)$	Objective function
x_i^*	Individual optimal
Y_j	Original response
$\hat{y}_{ij}$	Pareto-optimal solutions
$\bar{\mathbf{\Phi}}$	Payoff matrix
r	Pearson correlation
σ_{Y_j}	Standardized deviation of the original response
$Z(\cdot)$	Standardized normal variable
ζ_{PC}	Target value of the principal component
ζ_{Y_j}	Target value of the original response
$\hat{\mathbf{n}}$	Unitary normal vector

to use non-trivial technical planning and quality improvement, rather than the analysis only by the experience of their operators or by specifications manufacturer. However, the correct choice of cutting parameters as well as the suitable machining technique is not an easy task since it requires that processes are prepared to simultaneously optimize more than one quality characteristic (Paiva et al., 2009). In this way, the optimization methods should identify a set of optimal solutions that matches the needs of the organization allowing the decision maker to choose the optimal alternative.

A traditional experimental strategy is to analyze the behavior of some desired features that are considered significant as a function of the factor's increment. However, as with most parts of the machining processes, also in milling, the multiple quality characteristics measured are highly correlated and, with different optimization objectives. In these cases, the individual analyses of each response may lead to a conflicting optimum, since the factor levels that improve one response can, otherwise, degrade another (Paiva et al., 2009). The presence of correlation or the use of optimization methods that do not consider it, can also cause the model's instability, the overfitting, and the inaccuracy on the regression coefficients (Bratchell, 1989; Paiva et al., 2009).

The optimization literature frequently reveals correlated responses and with conflicting objectives in various milling studies. It happens mainly when the material removal rate and surface roughness are considered in the same analysis (Chahal et al., 2013; Jozić et al., 2015; Moshat et al., 2010; Singh et al., 2014; Thangarasu et al., 2012; Yan and Li, 2013). In all these studies, a strong, moderated correlation with significant statistic among the responses was observed (this analysis was carried out by us, using the Pearson Correlation, r). Although the results found have been coherent, the correlation structure was not considered or mentioned in these works. Just a study has assumed that correlated responses could deviate the optimization results (Moshat et al., 2010). In fact, Paiva et al. (2009) state that few studies have been published covering traditional methods when the responses are correlated.

The correlation influence becomes also important in the context of Pareto Frontiers. Since the frontier is obtained by a weighting process among the two or more objective function, if the correlation is strong and if it is neglected, the weights promote a separation that does not exist in practice. In other words, it can yield an excellent Pareto Frontier composed by unrealistic feasible solutions.

Normal Boundary Intersection (NBI) (Das and Dennis, 1998), is a multi-objective optimization method developed mainly to compensate the shortcomings attributed to the method of Weighted Sums (WS) such as its inability to find a uniform spread of Pareto optimal solutions, mainly when the multi-objective problem is non-convex. For these reasons, becomes NBI method a very useful option in optimizing many industrial processes with multiple responses. However, if multiples functions are correlated and with conflicting objectives, the NBI method tends to fail and the optimization's results can produce unreal values. Additionally, convex Pareto-optimal of solutions is not guaranteed since the influence of weights work in the attempt of separate the correlated objective functions.

To overcome this drawback, the Pareto frontier may be designed with uncorrelated objective functions. This procedure can be done using a multivariate statistical technique called Multivariate Mean Square Error (MMSE), developed by Paiva et al. (2009), that combines the Response Surface Methodology (RSM) (Box and Draper, 1987), the Principal Components Analysis (PCA) (Bratchell, 1989) and the concept of Mean Square Error (MSE) (Lin and Tu, 1995). The MMSE method is able to convert the original multiple correlated objective functions in a new set of uncorrelated ones, while

ARTICLE IN PRESS

considering the respective targets. Once modeled, the objective functions may be optimized by NBI method, which in turn often leads to continuous Pareto frontier.

Given the aforementioned discussion this work presents a multi-objective hybrid approach, called NBI-MMSE, that integrates the Normal Boundary Intersection method with the Multivariate Mean Square Error method for correlated multiple responses. To illustrate this proposal, a case study of AISI 1045 steel dry end milling process is used. The optimization by the Weighted Sum method with MMSE (called WS-MMSE) was carried out under the same process. The objective of process parameters optimization is to achieve at the same time the maximum volume of removed material and minimum surface roughness. The optimization results will be validated statistically to confirm the adequacy of the work's proposal.

2. Normal boundary intersection method vs. weighted sums for multi-objective optimization with multivariate mean square error functions

The idea of Weighted Sums method is to convert the multi-objective optimization into a single objective optimization problem, giving to each objective function $f_i(x)$ a different weight (w) (Das and Dennis, 1998), as:

$$\begin{aligned}&\min_{x} \sum_{i=1}^{n} w_i f_i(x) = w^T F(x)\\&s.t: x \in C\end{aligned} \tag{1}$$

However, if the Pareto set is non-convex, the Pareto points on the concave parts of the trade-off surface will be missed, and instead, they will cluster in regions with strong curvature (Brito et al., 2014). In order to overcome the disadvantages of WS method, Das and Dennis (1998) proposed the Normal Boundary Intersection method. The authors proved that the NBI method is independent of the relative scales of the functions and it is successful in producing an evenly distributed set of points in the Pareto set.

The first step in the NBI method, according to Das and Dennis (1998), comprehends the establishment of payoff matrix ($\overline{\boldsymbol{\Phi}}$), based on the calculation of the individual minima of each objective function. The solution that minimizes the i-th objective function $f_i(x)$ can be represented as$f_i^*(x_i^*)$. When we replace the individual optimal (x_i^*) in the remaining objective functions we have$f_i(x_i^*)$. In matrix notation, the $\overline{\boldsymbol{\Phi}}$ can be written as:

$$\overline{\boldsymbol{\Phi}} = \begin{bmatrix} f_1^*(x_1^*) & \cdots & f_1(x_i^*) & \cdots & f_1(x_m^*) \\ \vdots & \ddots & & & \vdots \\ f_i(x_1^*) & \cdots & f_i^*(x_i^*) & \cdots & f_i(x_m^*) \\ \vdots & & & \ddots & \vdots \\ f_m(x_1^*) & \cdots & f_m(x_i^*) & \cdots & f_m^*(x_m^*) \end{bmatrix} \tag{2}$$

Each row of the payoff matrix $\overline{\boldsymbol{\Phi}}$ is composed by minimum $f_i^*(x_i^*)$ and maximum $f_i(x_i^*)$ values of the i-th objective function $f_i(x)$. These values can be used to normalize the objective functions, mainly when they will be written in terms of different scales or units. Likewise, writing a vector with the set of individual minimum$f^U = \left[f_1^*(x_1^*) \quad \ldots, \quad f_i^*(x_i^*) \quad \ldots, \quad f_m^*(x_m^*)\right]^T$, the Utopia point is obtained. Utopia point $f_i^*(x_i^*)$ is a specific point, generally outside of the feasible region, that corresponds to all objectives simultaneously being at their best possible values. Analogously, joining the maximum values of each objective function, $f^N = \left[f_i(x_i^*) \quad \ldots, f_i(x_i^*) \ldots, f_i(x_i^*)\right]^T$, the Nadir point $f_i(x_i^*)$ is obtained. It's the design space where all objectives are simultaneously at their worst values. The two anchor points connected by Utopia line are obtained when the i-th objective is minimized independently (Brito et al., 2014). The normalization of the objective functions can be obtained using these two sets, such as:

$$\bar{f}(x) = \frac{f_i(x) - f_i^U}{f_i^N - f_i^U}, i = 1, \ldots, m \tag{3}$$

This normalization leads to scalarization of the $\overline{\boldsymbol{\Phi}}$ and the vector$\overline{\mathbf{F}}(\mathbf{x})$. Associated to vector of weights ($\boldsymbol{\beta}$) and a unitary normal vector($\widehat{\mathbf{n}}$), the classical NBI formulation can be described as:

$$\begin{aligned}&\underset{(\mathbf{x},t)}{Max}\ D\\&S.t: \overline{\boldsymbol{\Phi}}\boldsymbol{\beta} + D\widehat{\mathbf{n}} = \overline{\mathbf{F}}(\mathbf{x})\\&\mathbf{x} \in \Omega\\&g_j(x) \le 0\\&h_j(x) \le 0\end{aligned} \tag{4}$$

The conceptual parameter (D) can be algebraically eliminated from Equation (4), such that, for bi-dimensional problem, this expression can be simplified as:

$$\begin{aligned}&Min\ \overline{f_1}(\mathbf{x})\\&s.t.: \overline{f_1}(\mathbf{x}) - \overline{f_2}(\mathbf{x}) + 2w - 1 = 0\\&g_j(\mathbf{x}) \ge 0\\&0 \le w \le 1\end{aligned} \tag{5}$$

where $\overline{f_1}(\mathbf{x})$ and $\overline{f_2}(\mathbf{x})$ are normalized objective functions, $g_j(\mathbf{x}) \ge 0$ and $0 \le w \le 1$ are the set of constraints for experimental region and the cuboidal region, respectively. In some cases it is appropriate to adopting both restrictions. This optimization problem can be iteratively solved for different values of weight (w) creating an evenly distributed Pareto frontier.

However, as previously mentioned, if several objective functions are positively correlated and present conflicting objectives among themselves, the NBI method tends to fail and to produce unreal results and no-convex frontiers. In order, to fill this gap, Paiva et al. (2009) proposed the MMSE method, which combines RSM, PCA and MSE. In doing so, the MMSE method obtains uncorrelated objective functions from the Principal Components, while considering the respective targets, as Equation (6).

$$MMSE_i = \left[(PC - \zeta_{PC})^2 + \lambda_{PC}\right], i = 1, 2, \ldots, p \tag{6}$$

with,

$$PC = b_{0i} + \left[\nabla f(\mathbf{x})^T\right]_i + \left\{\frac{1}{2}\mathbf{x}^T\left[\nabla^2 f(\mathbf{x})\right]\mathbf{x}\right\}_i, i = 1, 2, \ldots, p \tag{7}$$

$$\zeta_{PC} = \sum_{j=1}^{p} e_{ij} \cdot \left[Z\left(Y_j \middle| \zeta_{Y_j}\right)\right], j = 1, 2, \ldots, p \tag{8}$$

where, i is the number of $MMSE_i$ function according with the number of significant i-th principal component (PC). According to Johnson and Wichern (2007), a PC is considered significant if the variance-covariance structure established among the original response is greater than 80%. In Equation (7), PC is defined as the fitted second-order polynomial positioned in relation to the input variables. ζ_{PC} is the target value of the i-th principal components that must keep a straightforward relation with the targets established for the original dataset. ζ_{PC} is defined according Equation (8), where $Z(Y_j|\zeta_{Y_j}) = [(\zeta_{Y_j}) - \mu_{Y_j}] \cdot (\sigma_{Y_j})^{-1}$ is the standardized normal variable $Z(\cdot)$ calculated for each original response (Y_j) considering, the Utopia point, the mean (μ_{Y_j}) and the standard deviation (σ_{Y_j}) of each Y_j. e_{ij} represents the eigenvector set associated to the i-th

Please cite this article in press as: Duarte Costa, D.M., et al., A normal boundary intersection with multivariate mean square error approach for dry end milling process optimization of the AISI 1045 steel, Journal of Cleaner Production (2016), http://dx.doi.org/10.1016/j.jclepro.2016.01.062

ARTICLE IN PRESS

principal component. Finally, λ_{PC} are the eigenvalues associated to the *PC*.

Once the $MMSE_i$ formulations are established the multi-objective problem can be resolved by NBI method. In general, the number of equations obtained to replace the original set is smaller than the initial amount, obviously depending on the strength of the variance-covariance structure (Paiva et al., 2009).

Thus, taking $f_i(x) = MMSE_i(x)$, $f_i^U = MMSE_i^U(x)$ and $f_i^N = MMSE_i^N(x)$ to developed multi-objective optimization by NBI-MMSE approach and, then, adopting the scalarization described by Equation (3), a bidimensional NBI method for $MMSE_i$ functions, with $i = 1,2,\ldots,p$ can be written as:

$$\begin{aligned} & Min\,\overline{f}_1(\mathbf{x}) = \left(\frac{MMSE_1(\mathbf{x}) - MMSE_1^U(\mathbf{x})}{MMSE_1^N(\mathbf{x}) - MMSE_1^U(\mathbf{x})}\right) \\ & s.t.: g_1(\mathbf{x}) = \left(\frac{MMSE_1(\mathbf{x}) - MMSE_1^U(\mathbf{x})}{MMSE_1^N(\mathbf{x}) - MMSE_1^U(\mathbf{x})}\right) - \left(\frac{MMSE_2(\mathbf{x}) - MMSE_2^U(\mathbf{x})}{MMSE_2^N(\mathbf{x}) - MMSE_2^U(\mathbf{x})}\right) + 2w - 1 = 0 \\ & g_2(\mathbf{x}) = \mathbf{x}^{\mathbf{T}}\mathbf{x} \le \rho \end{aligned} \tag{9}$$

where, $MMSE_1(\mathbf{x})$ and $MMSE_2(\mathbf{x})$ are calculated as suggested by Paiva et al. (2009). $MMSE_i^U(\mathbf{x})$ were determinate by individual constraint minimization, such as $MMSE_i^U(\mathbf{x}) = \underset{\mathbf{x}\in\Omega}{Min}[MMSE_i(\mathbf{x})]$, where Ω denotes the experimental region in which $\mathbf{x}$ is inserted. The denominator $MMSE_i^N(\mathbf{x}) - MMSE_i^U(\mathbf{x})$ is used to normalize the multiple responses, doing $MMSE_i^N(\mathbf{x})$ as the maximum value of payoff matrix (matrix formed by all solutions observed in the individual optimizations). The set of constraints$g_2(\mathbf{x}) = \mathbf{x}^{\mathbf{T}}\mathbf{x} \le \rho^2$, where ρ is the design radius, represents the experimental region, but, other constraints can be added if it is necessary. In terms of design factors, this proposal establishes the empirical models for multiple responses of dry end milling process, but can be used in any manufacturing process.

Once the multi-objective function is established, its optimum can be generally reached by using Generalized Reduced Gradient (GRG). GRG is considered one of the most robust and efficient gradient algorithms for nonlinear.

To the better understanding of the NBI-MMSE approach proposed in this work a step-by-step procedure was developed and can be seen in the next section.

3. Proposed procedure for dry end milling process optimization of the AISI 1045 steel using NBI-MMSE approach

The multi-objective optimization of dry end milling process by employing NBI-MMSE approach for multi-correlated responses was conducted in three stages. In the first stage, a Central Composite Design (CCD) using Response Surface Methodology (RSM) is proved to determine and model the objective functions for the original responses, as such Surface roughness arithmetic average surface roughness (R_a), maximum surface roughness (R_y), root mean square roughness (R_q), ten point height roughness (R_z), maximum peak to valley (R_t) and material removal rate (MRR). In the second stage, the correlation structure among responses is analyzed. If confirmed the dependence relationship among the multiple responses, in third stage, the NBI-MMSE approach is applied according the step-by-step follows:

Step a: Conduct the PCA on the original responses (Y_j) using the correlation matrix. Define the number of significant *i*-th principal component (*PC*) that must be retained in the analysis to compose the $MMSE_i$ function, and store their respective scores (*PC-scores*), eigenvalues (λ_{PC}) and eigenvectors (e_{ij}). Then, determine the quadratic models for the significant *PC*;

Step b: Establish the Utopia (f_i^U) and Nadir (f_i^N) point of each original response (Y_j), using the individual constraint minimization, such as $f^U(Y_j) = \underset{\mathbf{x}\in\Omega}{Min}\,[\widehat{Y}_j(\mathbf{x})]$(or maximization, such as$f^N(Y_j) = \underset{\mathbf{x}\in\Omega}{Max}[\widehat{Y}_j(\mathbf{x})]$). The calculated Utopia point was considered as the target (ζ_{Yj}) and Nadir point as specification limit, for the optimization problem;

Step c: Using the *PC-scores* obtained in Step a, the target of the each principal components (ζ_{PC}) and their respective eigenvalue (λ_{PC}), calculate the $f_i(\mathbf{x}) = MMSE_i(\mathbf{x})$ function according Equation (6). Remember that the number of $MMSE_i$ function used in the NBI-MMSE approach will be dependent on the number of significant principal components. Then, determine the quadratic models using Ordinary Least Squares (OLS) algorithm;

Step d: Take the $MMSE_i$ function developed in Step c and obtain the values of $MMSE_i^U(\mathbf{x})$ and $MMSE_i^N(\mathbf{x})$. Afterward, develop Payoff matrix $\overline{\mathbf{\Phi}}$ with both values. For a bi-objective case, $\overline{\mathbf{\Phi}}$ can be written as Equation (10). With the values of the $\overline{\mathbf{\Phi}}$, develop its scalarization, as such Equation (11);

$$\overline{\mathbf{\Phi}} = \begin{bmatrix} MMSE_1^U(\mathbf{x}) & MMSE_1^N(\mathbf{x}) \\ MMSE_2^N(\mathbf{x}) & MMSE_2^U(\mathbf{x}) \end{bmatrix} \tag{10}$$

$$\begin{aligned} & \bar{f}(x) = \frac{f_i(x) - f_i^U}{f_i^N - f_i^U} \Rightarrow \left\{ \begin{aligned} & \bar{f}_1(x) = \overline{MMSE_1}(\mathbf{x}) = \frac{MMSE_1(\mathbf{x}) - MMSE_1^U}{MMSE_1^N - MMSE_1^U} \\ & \bar{f}_2(x) = \overline{MMSE_2}(\mathbf{x}) = \frac{MMSE_2(\mathbf{x}) - MMSE_2^U}{MMSE_2^N - MMSE_2^U} \end{aligned} \right\} \\ & \bar{f}(x) = \frac{f_i(x) - f_i^U}{f_i^N - f_i^U} \Rightarrow \left\{ \begin{aligned} & \bar{f}_1(x) = \overline{MMSE_1}(\mathbf{x}) = \frac{MMSE_1(\mathbf{x}) - MMSE_1^U}{MMSE_1^N - MMSE_1^U} \\ & \bar{f}_2(x) = \overline{MMSE_2}(\mathbf{x}) = \frac{MMSE_2(\mathbf{x}) - MMSE_2^U}{MMSE_2^N - MMSE_2^U} \end{aligned} \right\} \end{aligned} \tag{11}$$

Step e: Solve the system of Equation (9) using GRG algorithm for different values of *w*, generally range [0;1] and constrained only to the experimental region. Create Pareto frontier.

Fig. 1 summarizes the proposed approach in this work.

4. Experimental procedure

4.1. Work piece material, machine tool, and cutting tool

In this investigation, AISI 1045 steel with hardness of approximately 180HB was selected as the workpiece material for dry end milling process. The dimensions of workpiece were rectangular

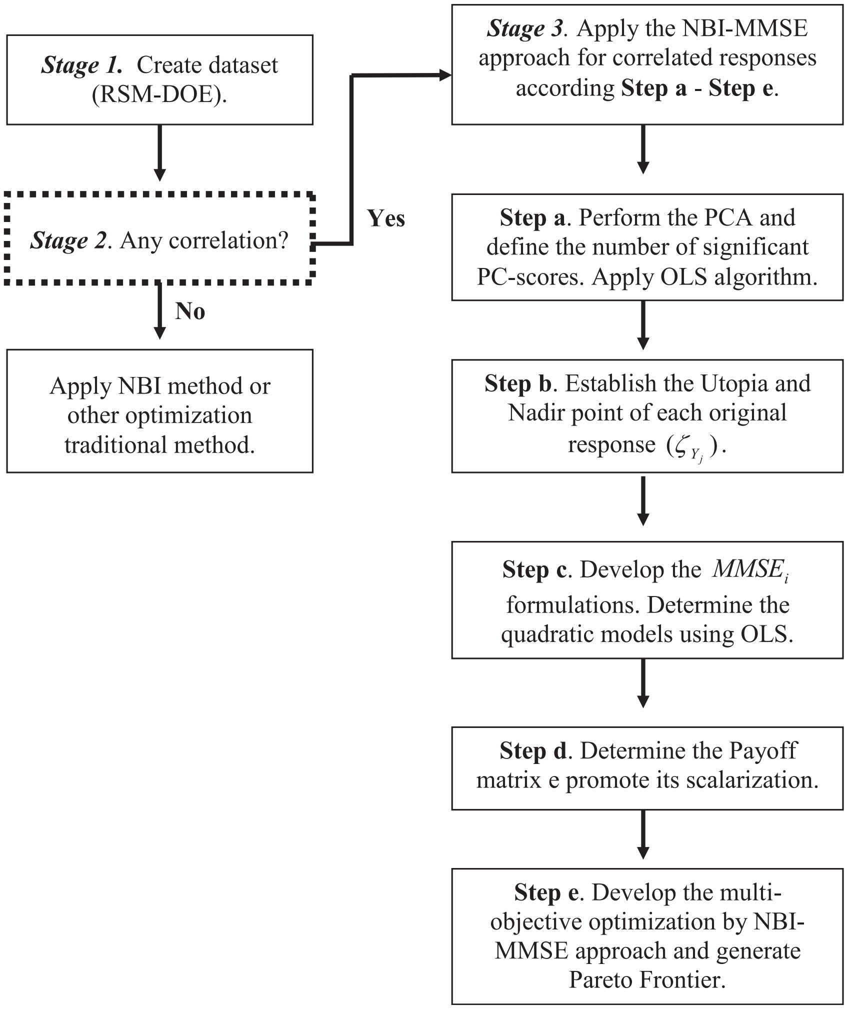

Fig. 1. Overview of the proposed NBI-MMSE approach.

blocks square sections of 100 × 100 mm and lengths of 300 mm. Table 1 shows the chemical composition of test sample fixed according to manufacturer's description.

The dry end milling experiments were conducted on a FADAL, vertical machining center, model VMC 15, having a maximum power of 15 kW and maximum rotation speed of 7500 RPM. The tool overhang was 60 mm. The tool used was a positive end mill, code R390-025A25-11M (Sandvik) with a 25 mm diameter (DC_{ap}), entering angle of $\chi_r - 90^\circ$, and a medium step with three inserts (Z). Three rectangular inserts, with edge lengths of 11 mm each, code R390-11T308M-PM GC 1025 (Sandvik), were used. The tool material used was cemented carbide ISO P10 coated with TiCN and TiN by the PVD process. The coating hardness was around 3000 HV3 and the substrate hardness 1650 HV3 with a grain size smaller than 1 μm. The surface roughness of the machined workpiece was measured using a Mitutoyo portable roughness meter, model Surftest SJ 201, with a cut-off length of 0.25 mm.

Table 1
Chemical composition of AISI 1045 steel.

Elemento	C	Mn	P_{max}	S_{max}
(%)	0.43–0.50	0.60–0.90	0.04	0.05

4.2. Design of experiments and experimental results

RSM is a collection of statistical and mathematical techniques which are useful for the modeling and analysis of problems in which a responses of interest are not known and are influenced by several variables (Box and Draper, 1987). In this study, RSM based on a CCD, was used in the experimental matrix.

According to Montgomery (2012), CCD spans a set of quantitative factors with fewer points than another design methodology, without a large loss in efficiency. According the author, CCD is a design widely used for estimating second-order response surface. The CCD involves (i) factorial point, at levels ±1, determined by 2^k, where k is number of controllable parameters present in the design, (ii) axial point, determined by $2k$, and (iii) center point (n). CCD presents also the value of each axial point from the center in a CCD. It is determined by $\alpha = \sqrt[4]{2^k}$. The factorial point represent a variance optimal design for the estimative of linear and interaction effects. The center points provide information about the existence of curvature in the system and your multiplying can improve the estimates of the quadratic effects and allow additional degrees of freedom for error (Montgomery, 2012).

To accomplish the aims of this work, the cutting parameters defined as input variables were the feed per tooth (f_z), axial depth of cut (a_p), Cutting speed (V_c) and radial depth of cut (a_e). The experimental matrix was based on CCD, created for four

Table 2
Cutting parameters and respective levels.

Cutting parameters	Levels (uncoded and coded)				
	−2	−1	0	+1	+2
feed per tooth (f_z, mm/tooth)	0.05	0.10	0.15	0.20	0.25
axial depth of cut (a_p, mm)	0.38	0.75	1.12	1.50	1.87
Cutting speed (V_c, m/min)	275	300	325	350	375
radial depth of cut (a_e, mm)	13.5	15.0	16.5	18.0	19.5

parameters, totaling 16 runs ($2^k = 2^4 = 16$), eight axial points ($2k = 8$), and six center points. This resulted in 30 experiments. In the CCD, a coded distance of 2.0 was adopted for the center points to the axial points. The software Minitab® was used to build the experimental matrix and to perform the statistical analysis from the experimental data.

To specify the parameter levels, preliminary tests were taken into account. For this, the values initially adopted cutting parameters correspond to the operational limits recommended by the toolmaker together with the machine tool capabilities. Then, the limits of each variable were pre-fixed and the preliminary tests were performed to verify the process behavior on the extreme conditions. At the end of this analysis, the parameter levels were fixed, as shown in Table 2.

The set of the responses included R_a, R_y, R_q, R_z, R_t and MRR. The five roughness responses are measured, while the MRR (cm^3/min), in end milling process, can be calculated as follows (Wang and Hsu, 2005):

$$MRR_i = \frac{V_{f_i} \cdot a_{p_i} \cdot a_{e_i}}{1,000} = \frac{f_z \cdot N \cdot Z \cdot a_p \cdot a_e}{1,000} \tag{12}$$

where i is the number of experiments, V_f is the table feed (mm/min), N is the spindle speed (RPM), and Z is the number of effective teeth of the tool (Z = 3). N can be calculated as $N_i = \frac{V_{c_i} \cdot 1000}{\pi \cdot DC_{ap}}$, where DC_{ap} is the cutting diameter at cutting depth, of the tool ($DC_{ap} = 25$ mm).

Once all the responses had been measured, they were assembled to compound the experimental matrix presented in Table 3.

5. Results and discussion

5.1. Model development

To analyzing the influence of cutting parameters (f_z, a_p, V_c, a_e) on the roughness responses and the MRR response, in dry end milling process, a second-order polynomial mathematical equation was used:

$$\begin{aligned} y(\mathrm{x}) = {} & \beta_0 + \beta_1 f_z + \beta_2 a_p + \beta_3 V_c + \beta_4 a_e + \beta_{11} f_z^2 + \beta_{22} a_p^2 + \beta_{33} V_c^2 + \beta_{44} a_e^2 + \\ & \beta_{12} f_z a_p + \beta_{13} f_z V_c + \beta_{14} f_z a_e + \beta_{23} a_p V_c + \beta_{24} a_p a_e + \beta_{34} V_c a_e + \varepsilon \end{aligned} \tag{13}$$

where, $\beta_0, \beta_1, \beta_2, \beta_3, \beta_4$ are coefficients to be estimated.

The Ordinary Least Squares (OLS) algorithm was applied to developing the full quadratic models of each response, as shown in Table 4. Table 5 presents the obtained coefficients for the final full quadratic models, the significance level of each term and the main results of the ANOVA.

All models presented adj. R^2 values above 90.0% indicating a good adequacy for all expressions and no lack of fit was observed. Feed per tooth and axial depth of cut are the most important factors to explain the behavior of all the responses. Although the other terms were not significant, they were kept in the model because their exclusion did not imply prediction variance reduction. The results of the normality test, for the residuals of the RSM models, demonstrated that the residuals are normal, since all Anderson–Darling coefficients were less than 1.000 (with p-values higher than 5% of significance). However, this was not observed for surface MRR, since the MRR is not an experimental response.

Table 5 also presents the curvature p-values calculated for the responses. All roughness responses presented a value less than 5% of significance. This means that the experimental space for these responses falls within the curvature region. As MRR is not an experimental response, there is no guarantee that the MRR equation will present curvature. Similarly, MRR equation presents no residual-error. Thus, Lack of fit cannot be calculated for MRR.

ANOVA results showed that all developed final full quadratic models are reliable and can be used for optimization of this end milling process.

Figs. 2 and 3 set forth the response surface for the responses (R_a and MRR, respectively) as function of all the cutting parameters: f_z, a_p, V_c and a_e.

5.2. Results of the end milling process optimization using NBI-MMSE approach and WS-MMSE

Before applying the NBI-MMSE approach it is necessary to analyze the correlation structure among the responses to be optimized. According to the correlation results presented in Table 6, it can be seen that R_a, R_y, R_q, R_z and R_t are objective functions highly correlated. It was observed also a positive, moderate correlation among roughness responses and MRR.

Since the surface roughness and MRR exhibit positive correlation and considering that these objective functions are conflicting, there is a tradeoff where the MMSE method could satisfactorily solve the problem.

As suggested in **Step a**, the PCA was next performed to find the uncorrelated principal components needed to represent the original responses of the NBI-MMSE approach. Using the correlation matrix, the PC's scores were extracted from the original responses and stored (Table 3) with their respective eigenvalues and eigenvectors (Table 7).

Considering that the first principal component (PC_1) represents 87.50% of variance covariance structure established among the original responses, the multi-objective function could be represented using only (PC_1). However, the eigenvectors show a highly positive relation between PC_1 and R_a, R_y, R_z, R_q and R_t, while a poor relation can be observed between PC_1 and the response MRR. On the other hand, although there is not a notably explanation in the second principal component (PC_2), there is a strong, positive relation between PC_2 and MRR, which suggest that PC_2 should also be taken into account. Just as observed by Paiva et al. (2009), these kind of relationship indicates that the minimization of the $MMSE_i$ functions (built only with PC_1) can be able to achieve all targets of optimized responses, but this doesn't happen to MRR response, i.e., examining the eigenvectors in Table 7, one can observe that is impossible to minimize roughness responses and minimize MRR

ARTICLE IN PRESS

Table 3
Experimental matrix and results.

Exp.No	Cutting Parameters				Original responses						Responses			
					Quality (μm)					Productivity (cm^3/min)	Minimize	Maximized	Minimize	Minimize
	f_z	a_p	V_c	a_e	R_a	R_y	R_z	R_q	R_t	MRR	PC_1	PC_2	$MMSE_1$	$MMSE_2$
1	0.10	0.750	300	15.00	1.18	5.53	5.16	1.37	5.63	12.89	−2.19	−0.82	13.57	26.38
2	0.20	0.750	300	15.00	1.98	9.71	8.86	2.34	10.04	25.78	3.27	−1.43	*	32.95
3	0.10	1.500	300	15.00	1.17	5.01	4.76	1.36	5.14	25.78	−2.37	0.04	12.56	18.40
4	0.20	1.500	300	15.00	1.48	7.89	7.00	1.82	7.94	51.57	1.03	0.90	42.60	11.88
5	0.10	0.750	350	15.00	1.15	4.75	4.44	1.31	4.76	15.04	−2.89	−0.54	10.03	23.63
6	0.20	0.750	350	15.00	2.08	9.27	8.74	2.43	9.48	30.08	3.25	−1.22	*	30.60
7	0.10	1.500	350	15.00	1.10	5.06	4.62	1.25	5.16	30.08	−2.52	0.39	11.82	15.55
8	0.20	1.500	350	15.00	1.69	8.05	7.39	2.00	8.30	60.16	1.86	1.19	53.37	10.05
9	0.10	0.750	300	18.00	1.04	5.78	4.78	1.21	5.85	15.47	−2.46	−0.51	12.11	23.31
10	0.20	0.750	300	18.00	1.67	8.03	7.65	2.06	8.17	30.94	1.43	−0.62	47.57	24.38
11	0.10	1.500	300	18.00	1.16	5.22	4.95	1.34	5.38	30.94	−2.15	0.34	13.85	15.97
12	0.20	1.500	300	18.00	1.82	9.13	8.18	2.19	9.27	61.88	3.00	1.02	*	*
13	0.10	0.750	350	18.00	1.19	5.33	5.13	1.37	5.49	18.05	−2.19	−0.50	13.58	23.21
14	0.20	0.750	350	18.00	1.99	8.86	8.32	2.35	8.88	36.10	2.78	−0.70	67.07	25.23
15	0.10	1.500	350	18.00	1.18	5.13	4.79	1.36	5.35	36.10	−2.09	0.65	14.18	13.64
16	0.20	1.500	350	18.00	1.74	8.52	7.48	2.07	8.74	72.19	2.46	1.83	62.09	6.54
17	0.05	1.125	325	16.50	0.37	2.68	2.00	0.45	2.73	11.52	−6.52	0.35	7.32	15.90
18	0.25	1.125	325	16.50	1.86	9.12	8.71	2.26	9.28	57.61	3.19	0.67	*	13.49
19	0.15	0.375	325	16.50	1.54	6.69	5.99	1.75	6.84	11.52	−0.55	−1.40	25.80	32.63
20	0.15	1.875	325	16.50	1.16	6.13	5.47	1.39	6.20	57.61	−1.03	1.85	21.62	6.42
21	0.15	1.125	275	16.50	1.55	7.18	6.54	1.80	7.34	29.25	0.24	−0.42	33.51	22.46
22	0.15	1.125	375	16.50	1.61	7.25	6.83	1.87	7.52	39.88	0.71	0.14	38.74	*
23	0.15	1.125	325	13.50	1.56	6.87	6.52	1.81	7.07	28.28	0.08	−0.46	31.89	22.90
24	0.15	1.125	325	19.50	1.60	7.09	6.72	1.85	7.49	40. 85	0.61	0.23	37.63	16.85
25	0.15	1.125	325	16.50	1.57	6.90	6.48	1.82	7.10	34.57	0.22	−0.09	33.30	19.51
26	0.15	1.125	325	16.50	1.63	7.22	6.81	1.90	7.39	34.57	0.62	−0.20	37.77	20.48
27	0.15	1.125	325	16.50	1.66	7.35	6.90	1.94	7.43	34.57	0.77	−0.24	39.46	20.88
28	0.15	1.125	325	16.50	1.59	7.25	6.59	1.83	7.39	34.57	0.45	−0.13	35.84	19.91
29	0.15	1.125	325	16.50	1.61	7.18	6.70	1.87	7.33	34.57	0.52	−0.17	36.56	20.20
30	0.15	1.125	325	16.50	1.61	7.18	6.69	1.85	7.32	34.57	0.49	−0.16	36.22	20.10
Mean (μ_{Y_j})					1.48	6.91	6.37	1.74	7.07	34.57	0.00	0.00	30.30	19.77
Standardized deviation (σ_{Y_j})					0.36	1.62	1.55	0.43	1.65	15.01	2.29	0.83	16.55	6. 82
Utopia point (ζ_{Y_j})					0.47	2.71	2.32	0.55	2.72	77.38	–	–	2.21	0.24
Standardized values $Z(Y_j\|\zeta_{Y_i})$					−2.86	−2.60	−2.62	−2.78	−2.63	2.74	–	–	–	–

* Denotes an observation with a large standardized residual..

simultaneously. In this way, the choice of the PC_1 and PC_2 to compose the NBI-MMSE approach can be responsible for the explanation of 98.90% of the variation structure of the six end milling responses (Table 7). In doing so, two uncorrelated objective functions of the principal components will be optimized by NBI-MMSE approach. Then, the OLS algorithm was applied and the final full quadratics models for PC_1 and PC_2 were developed (Table 4). Adj. R^2 values above 90.0% and no lack of fit was observed for both models (Table 5).

In **Step b**, the Utopia and Nadir point of each original response were determinate by individual constraint minimization (for roughness responses) and individual constraint maximization (for MRR response), such as $f^U(Y_j) = \underset{\mathbf{x}\in\Omega}{Min}[\widehat{Y}_j(\mathbf{x})]$ and $f^N(Y_j) = \underset{\mathbf{x}\in\Omega}{Max}[\widehat{Y}_j(\mathbf{x})]$, respectively. As previously mentioned, the. calculated Utopia points were considered as the target (ζ_{Yj}) of the original responses and Nadir point as specification limits for the optimization problem, i.e., the optimal values obtained by the optimization problem must lie between these two metrics. Table 8 shows the calculated Utopia and Nadir point for R_a, R_y, R_z, R_q, R_t and MRR.

In **Step c**, based on Equation (6) and considering the RSM models for PC_1 and PC_2, the $MMSE_i$ functions used in the NBI-MMSE approach were developed such as:

$$MMSE_1 = \left[(PC_1 - \zeta_{PC1})^2 + \lambda_{PC1}\right] \tag{24}$$

$$MMSE_2 = \left[(PC_2 - \zeta_{PC2})^2 + \lambda_{PC2}\right] \tag{25}$$

with,

$$\begin{aligned}\zeta_{PC} = {} & e_1[Z(R_a|\zeta_{Ra})] + e_2\left[Z\left(R_y|\zeta_{Ry}\right)\right] + e_3[Z(R_z|\zeta_{Rz})] \\ & + e_4\left[Z\left(R_q|\zeta_{Rq}\right)\right] + e_5[Z(R_t|\zeta_{Rt})] + e_6[Z(MRR|\zeta_{MRR})]\end{aligned} \tag{26}$$

Where, PC_1 and PC_2 are the scores of the principal components described in Table 3. Using the relationship established by Equation (26), the targets expressed in terms of principal components were calculated, resulting in $\zeta_{PC_1} = 5.079$ and $\zeta_{PC_2} = 4.250$. From Table 7, the eigenvalues of the each principal components are $\lambda_{PC_1} = 5.250$ and $\lambda_{PC_2} = 0.683$. The values of μ_{Y_j},σ_{Y_j},ζ_{Y_j} and standardized values $(Z(Y_i|\zeta_{Yi}))$ for each original responses (R_a, R_y, R_q, R_z, R_t and MRR) are cited in the four last lines of Table 3. Finally, e_{ij} represents the eigenvectors associated with their respective PC and its numerical values are described in Table 7.

The calculated values for $MMSE_1$ and $MMSE_2$ are cited in Table 3. As has been mentioned, the MMSE method obtains uncorrelated objective functions from the PC ($r = -0.265$, p-value $= 0.273$).

The final full quadratic models were developed for $MMSE_1$ and $MMSE_2$, as can be seen in Table 4 (Equations (22) and (23), respectively). The results showed in Table 5 indicate that all expressions are adequate, since the models presented adj. R^2 values

Please cite this article in press as: Duarte Costa, D.M., et al., A normal boundary intersection with multivariate mean square error approach for dry end milling process optimization of the AISI 1045 steel, Journal of Cleaner Production (2016), http://dx.doi.org/10.1016/j.jclepro.2016.01.062

Table 4
Full quadratic models for the responses.

$$R_a = 1.612 + 0.344f_z - 0.071a_p + 0.031V_c + 0.002a_e - 0.113f_z^2 - 0.054a_p^2 + 0.004V_c^2 + 0.004a_e^2 - 0.065f_za_p + 0.030f_zV_c + 0.001f_za_e - 0.029a_pV_c + 0.060a_pa_e + 0.013V_ca_e \quad (14)$$

$$R_y = 7.180 + 1.689f_z - 0.182a_p - 0.050V_c + 0.049a_e - 0.265f_z^2 - 0.138a_p^2 + 0.063V_c^2 + 0.005a_e^2 - 0.082f_za_p + 0.076f_zV_c - 0.093f_za_e + 0.022a_pV_c + 0.203a_pa_e + 0.043V_ca_e \quad (15)$$

$$R_z = 6.694 + 1.600f_z - 0.206a_p + 0.006V_c + 0.030a_e - 0.286f_z^2 - 0.192a_p^2 + 0.047V_c^2 + 0.030a_e^2 - 0.196f_za_p + 0.057f_zV_c - 0.064f_za_e - 0.049a_pV_c + 0.184a_pa_e + 0.047V_ca_e \quad (16)$$

$$R_q = 1.869 + 0.430f_z - 0.0741a_p + 0.025V_c + 0.006a_e - 0.113f_z^2 - 0.059a_p^2 + 0.007V_c^2 + 0.006a_e^2 - 0.072f_za_p + 0.027f_zV_c + 0.006f_za_e - 0.032a_pV_c + 0.062a_pa_e + 0.016V_ca_e \quad (17)$$

$$R_t = 7.326 + 1.715f_z - 0.179a_p - 0.037V_c + 0.063a_e - 0.282f_z^2 - 0.153a_p^2 + 0.074V_c^2 + 0.037a_e^2 - 0.101f_za_p + 0.076f_zV_c - 0.130f_za_e + 0.056a_pV_c + 0.233a_pa_e + 0.053V_ca_e \quad (18)$$

$$MRR = 34.565 + 11.522f_z + 11.522a_p + 2.659V_c + 3.142a_e + 0.000f_z^2 + 0.000a_p^2 + 0.000V_c^2 + 0.000a_e^2 + 3.841f_za_p + 0.886f_zV_c + 1.047f_za_e + 0.886a_pV_c + 1.047a_pa_e + 0.242V_ca_e \quad (19)$$

$$PC_1 = 0.510 + 2.390f_z - 0.114a_p + 0.086V_c + 0.100a_e - 0.473f_z^2 - 0.255a_p^2 + 0.061V_c^2 + 0.029a_e^2 - 0.187f_za_p + 0.134f_zV_c - 0.052f_za_e - 0.044a_pV_c + 0.319a_pa_e + 0.073V_ca_e \quad (20)$$

$$PC_2 = -0.165 + 0.106f_z + 0.801a_p + 0.137V_c + 0.183a_e + 0.149f_z^2 + 0.078a_p^2 - 0.013V_c^2 - 0.008a_e^2 + 0.321f_za_p + 0.017f_zV_c + 0.073f_za_e + 0.084a_pV_c - 0.023a_pa_e - 0.005V_ca_e \quad (21)$$

$$MMSE_1 = 36.523 + 20.125f_z - 0.992a_p + 2.652V_c + 1.500a_e + 2.086f_z^2 - 3.541a_p^2 0.437V_c^2 - 0.778a_e^2 - 1.355f_za_p + 3.633f_zV_c + 0.815f_za_e - 0.171a_pV_c + 0.592a_pa_e + 1.198V_ca_e \quad (22)$$

$$MMSE_2 = 20.179 - 0.716f_z - 6.833a_p - 0.623V_c - 1.799a_e - 1.312f_z^2 - 0.105a_p^2 + 0.376V_c^2 - 0.017a_e^2 - 2.853f_za_p + 0.321f_zV_c - 0.962f_za_e - 0.139a_pV_c + 0.237a_pa_e + 0.540V_ca_e \quad (23)$$

above 95.0% and no lack of fit were found. All the residuals are normal. Fig. 4 illustrates the overlaid contour graphics built for $MMSE_1$ and $MMSE_2$ and their responses surface in relation to each cutting parameters.

Since that the preceding steps have been performed, the multi-objective optimization by Normal Boundary Intersection, based on Multivariate Mean Square Error method can be developed.

In **Step d**, an individual constraint minimization for $MMSE_1$ and $MMSE_2$ were conducted, obtaining the values of Utopia point $MMSE_i^U(\mathbf{x})$ and Nadir $MMSE_i^N(\mathbf{x})$ for both the formulations. These values lead to the Payoff matrix $\overline{\mathbf{\Phi}}$ according to Equation (27). With the values of Payoff matrix, the scalarization of Payoff matrix based on Equation (11) was obtained.

$$\overline{\mathbf{\Phi}} = \begin{bmatrix} 2.209 & 53.874 \\ 18.250 & 0.237 \end{bmatrix} \quad (27)$$

Finally, in **Step e**, employing the GRG algorithm available from Microsoft Excel's Solver® routine for the system of equations (9), the minimization the values of $MMSE_1$ and $MMSE_2$ through NBI-MMSE approach produced values of roughness and MRR as can be seen in Table 9. Increments of approximately 5% were adopted in the weight (w) distribution. The experimental region constraint $\mathbf{x^Tx} \leq \rho^2$ was used. For a CCD, logical choice is $\rho = \alpha$, where α is the axial distance. Thus, the nonlinear constraint $\mathbf{x^Tx} \leq 4$ was considered since the axial distance (α) for CCD is 2.

For the sake of comparison, the same procedure was repeated using the Weighted Sums method for $MMSE_i$ functions (WS-MMSE) and the results are described in Table 10.

Such data established the Pareto frontier with NBI-MMSE approach and WS-MMSE approach, as given in Fig. 5 (a) and 5 (b), respectively.

It can be noted that the NBI-MMSE approach outperforms the WS-MMSE as a convex and equispaced frontier, avoiding the agglomeration of Pareto-optimal solutions along the frontier. Note that the Weighted Sums method forms a cluster of non-dominated solutions for $3.24 \leq MMSE_1 \leq 8.58$ and $11.93 \leq MMSE_2 \leq 15.88$. It is emphasized that in regions where the Weighted Sums method is incapable of finding feasible solutions, creating a discontinuity, the NBI-MMSE method generates a good deal of equispaced points.

All 21 Pareto solutions can be considered optimal solutions. However, in order to determine the optimal point of each approach to design confirmations experiments, the point that presented simultaneously the smaller roughness values and higher MRR values was selected. The sum of Least Square method, as such $SLS = \sum_{i=1}^{N}(f_{MMSE_i} - \mathrm{MMSE_i^U})^2$, where $i = 1{,}2$, was taken as

Table 5
Estimated coefficients for the quadratic models and ANOVA results.

Coefficient	R_a	R_y	R_z	R_q	R_t	MRR	PC_1	PC_2	$MMSE_1$	$MMSE_2$
Constant	**1.61**	**7.18**	**6.69**	**1.87**	**7.33**	**34.57**	**0.51**	**−0.17**	**36.52**	**20.18**
f_z	**0.34**	**1.69**	**1.60**	**0.43**	**1.72**	**11.52**	**2.39**	**0.11**	**20.12**	**−0.72**
a_p	**−0.07**	**−0.18**	**−0.21**	**−0.07**	**−0.18**	**11.52**	−0.11	**0.80**	−0.99	**−6.83**
V_c	0.03	−0.05	0.01	0.02	−0.04	**2.66**	0.09	**0.14**	**2.65**	**−0.62**
a_e	0.00	0.05	0.03	0.01	0.06	**3.14**	0.10	**0.18**	**1.50**	**−1.80**
f_z^2	**−0.11**	**−0.27**	**−0.29**	**−0.11**	**−0.28**	0.00	**−0.47**	**0.15**	**2.09**	**−1.31**
a_p^2	**−0.05**	−0.14	**−0.19**	**−0.06**	−0.15	0.00	**−0.25**	**0.08**	**−3.54**	−0.10
V_c^2	0.00	0.06	0.05	0.01	0.07	0.00	0.06	−0.01	−0.44	**0.38**
a_e^2	0.00	0.00	0.03	0.01	0.04	0.00	0.03	−0.01	−0.78	−0.02
f_z x a_p	**−0.07**	−0.08	**−0.20**	**−0.07**	−0.10	**3.84**	−0.19	**0.32**	−1.35	**−2.85**
f_z x V_c	0.03	0.08	0.06	0.03	0.08	**0.89**	0.13	0.02	**3.63**	0.32
f_z x a_e	0.00	−0.09	−0.06	0.01	−0.13	**1.05**	−0.05	**0.07**	0.82	**−0.96**
a_p x V_c	−0.03	0.02	−0.05	−0.03	0.06	**0.89**	−0.04	**0.08**	−0.17	−0.14
a_p x a_e	**0.06**	**0.20**	**0.18**	**0.06**	**0.23**	**1.05**	**0.32**	−0.02	0.59	0.24
V_c x a_e	0.01	0.04	0.05	0.02	0.05	0.24	0.07	−0.01	1.20	**0.54**
Adj. R^2 (%)	93.84	92.78	94.32	95.11	92.94	99.89	95.26	97.38	97.25	98.64
Lack of fit	0.07	0.08	0.05	0.09	0.05	[a]	0.05	007	0.17	0.09
Standard error	0.09	0.43	0.37	0.09	0.44	0.5	0.50	0.13	2.75	0.69
Regression p-value	0.00	0.00	0.00	0.00	0.00	0.00	0.00	0.00	0.00	0.00
Normality (AD) test	0.31	0.51	0.33	0.26	0.55	2.53	0.54	0.44	0.31	0.21
Normality (AD) p-value	0.54	0.12	0.51	0.68	0.14	<5%	0.16	0.27	0.53	0.84
Curvature p-value	0.00	0.00	0.00	0.00	0.00	[b]	0.00	0.00	0.02	0.00

Note: Bold values represent the individually significant terms (p-value<5%).
[a] Lack of fit cannot be calculated.
[b] Curvature cannot be calculated.

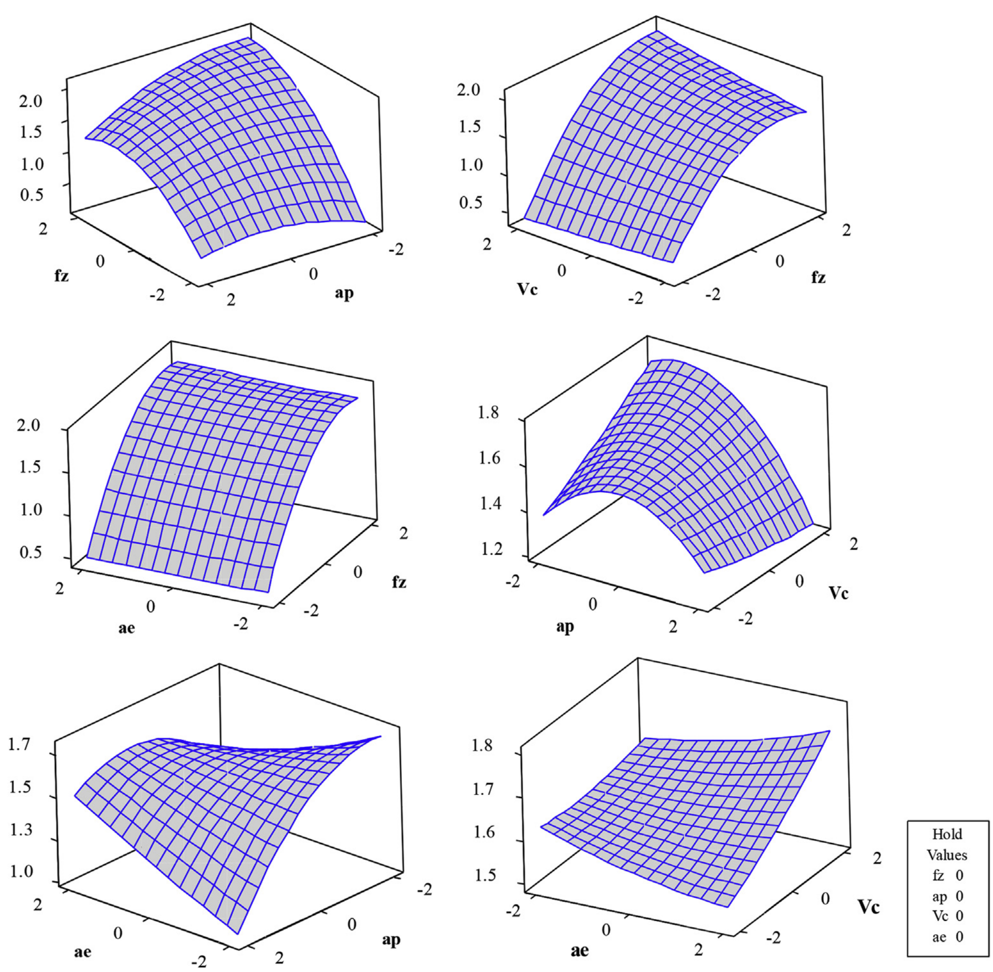

Fig. 2. Response surfaces for R_a in function of the end milling parameters.

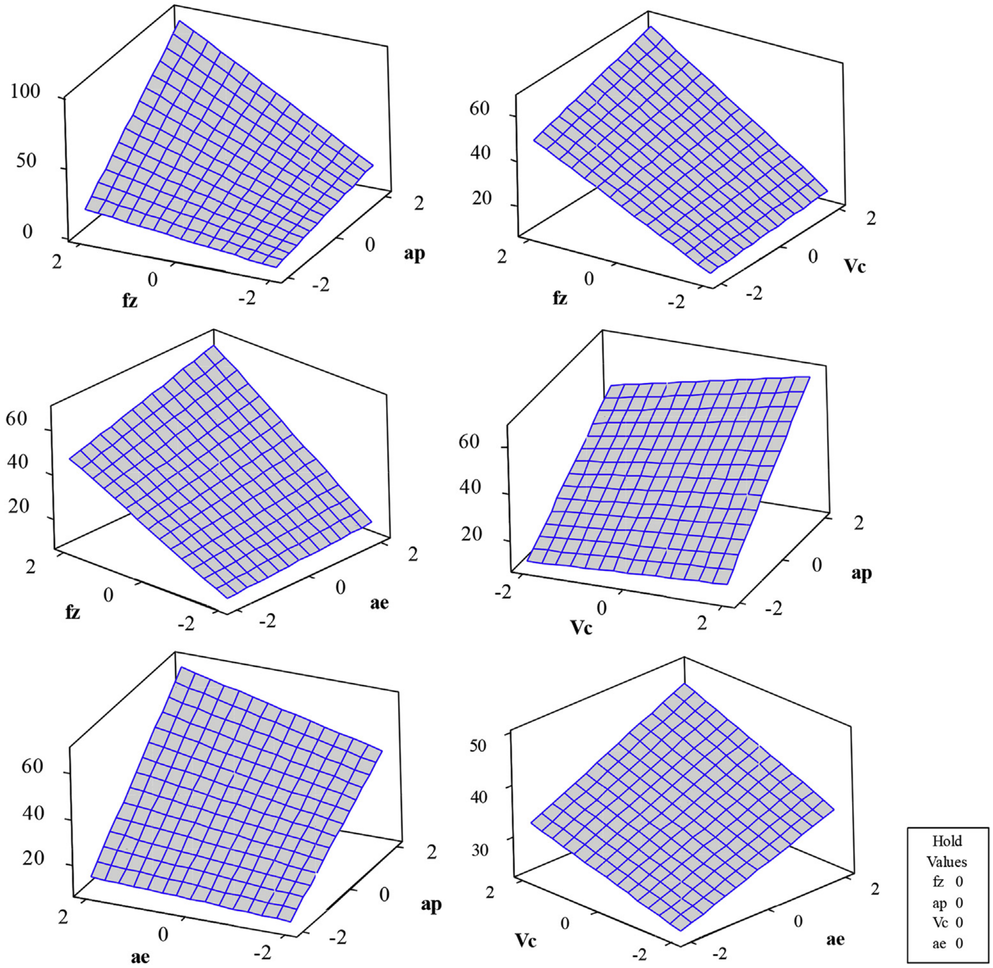

Fig. 3. Response surfaces for MRR in function of the end milling parameters.

Table 6
Correlation structure among original responses.

	R_a	R_y	R_z	R_q	R_t
R_y	0.956 (0.000)				
R_z	0.976 (0.000)	0.990 (0.000)			
R_q	0.996 (0.000)	0.972 (0.000)	0.990 (0.000)		
R_t	0.955 (0.000)	0.999 (0.000)	0.990 (0.000)	0.969 (0.000)	
MRR	0.481 (0.023)	0.557 (0.007)	0.512 (0.015)	0.508 (0.016)	0.561 (0.007)

Table 7
Principal Component Analysis for the end milling responses.

Eigenvalue (λ_{PC})	5.250	0.683	0.057
Proportion	0.875	0.114	0.010
Cumulative	0.875	0.989	0.999
Eigenvectors (e_{ij})	PC_1	PC_2	PC_3
R_a	0.425	−0.212	0.601
R_y	0.433	−0.057	−0.493
R_z	0.434	−0.105	−0.106
R_q	0.430	−0.165	0.392
R_t	0.433	−0.056	−0.462
MRR	0.268	0.954	0.133

criterion. The goal is to find values of $f_{(MMSEi)}$ that minimize the error. The two selected optimal points are presented in Table 11 and can be compared with the target (ζ_{Yj}) of the original responses.

Table 8
Utopia and Nadir points of the original responses.

	Utopia point	Nadir point
R_a	0.47	1.62
R_y	2.71	8.47
R_z	2.32	7.47
R_q	0.55	1.96
R_t	2.72	8.60
MRR	77.38	10.91

Comparing both selected optimal points ($w = 0.8$ and $w = 0.4$), it can be noted that to maximize the MRR while minimizing surface quality simultaneously, $f_z = 0.09$ mm/tooth, $a_p = 1.73$ mm, $V_c = 333.78$ m/min and $a_e = 16.20$ mm are the values that attained the desired quality conditions using the NBI-MMSE approach for end milling without cutting fluids. The following optimal levels of cutting parameters were found considering the multi-objective optimization by WS-MMSE carried out under the same process: $f_z = 0.10$ mm/tooth, $a_p = 1.76$ mm, $V_c = 332.00$ m/min and $a_e = 16.24$ mm.

Although axial depth of cut (a_p) has shown values above of the calculated parameters levels (±1), it can be observed that all optimized responses were established within the specification limits, which suggest it seems to be a good solution of the proposed approach for this case study.

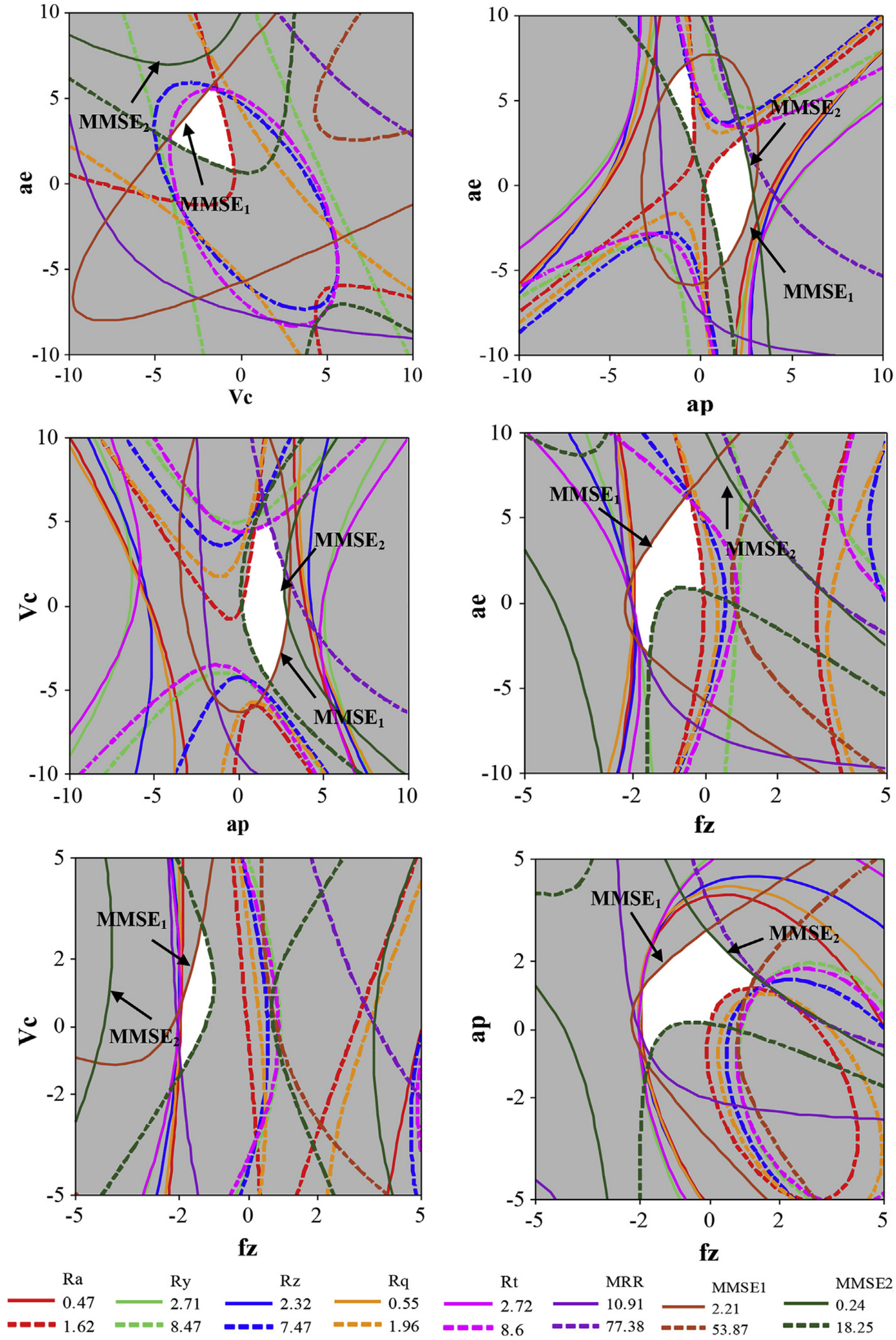

Fig. 4. Overlaid contour graphics.

6. Confirmation experiments

Before designing and running confirmation experiments, power and sample size capabilities were evaluated to ensure enough certainty detecting differences of magnitude between the selected optimal points for R_a, R_y, R_z, R_q and R_t using NBI-MMSE approach and WS-MMSE approach. Thus, considering a reliability of 95%, a series of 28 experiments were run under optimal experimental conditions found for NBI-MMSE approach (f_z = 0.09 mm/tooth, a_p = 1.73 mm, V_c = 333.78 m/min and a_e = 16.20 mm) and WS-MMSE (f_z = 0.10 mm/tooth, a_p = 1.76 mm, V_c = 332.00 m/min and a_e = 16.24 mm). For this, were machined $i = 7$ steps on the workpiece, measuring $M = 4$ repetitions in each step. At the end, 56 experiments were carried. Table 12 shows the confirmation test's results for NBI-MMSE and WS-MMSE. It can be seen that all the confirmation test's responses were established within the confidence interval (95% CI), and all experimental responses presented real values close to the predicted ones. The largest difference among the real values and predicted were found to WS-MMSE, occurring R_a and R_q, equaled 8.74 and 6.54%, respectively. As MRR response is calculated, this analysis is not necessary.

In addition to the mentioned analyses, Table 13 shows the results from One-way ANOVA comparing the differences among the means the experimental responses for the property NBI-MMSE approach and WS-MMSE. In One-way ANOVA, p-value < 0.05

Table 9
Pareto-optimal solutions for NBI-MMSE approach.

w	Uncoded parameters				Uncoded responses						$f_{(MMSE_1)}$	$f_{(MMSE_2)}$
	F_z	A_p	V_c	A_e	R_a	R_y	R_z	R_q	R_t	MRR		
0.00	**0.21**	**1.70**	**325.75**	**17.06**	**1.55**	**8.21**	**7.20**	**1.88**	**8.31**	**76.09**	**53.87**	**0.24**
0.05	0.21	1.73	324.87	17.03	1.52	8.02	7.02	1.84	8.11	75.11	49.06	0.36
0.10	**0.20**	**1.77**	**324.27**	**16.98**	**1.49**	**7.83**	**6.84**	**1.80**	**7.92**	**73.84**	**44.77**	**0.66**
0.15	0.19	1.79	323.87	16.94	1.46	7.64	6.67	1.76	7.73	72.35	40.86	1.10
0.20	0.19	1.82	323.62	16.89	1.43	7.45	6.51	1.72	7.55	70.67	37.24	1.64
0.25	0.18	1.83	323.54	16.84	1.41	7.26	6.34	1.68	7.36	68.82	33.87	2.27
0.30	0.17	1.85	323.59	16.79	1.38	7.07	6.18	1.65	7.16	66.79	30.70	2.97
0.35	0.17	1.86	323.75	16.73	1.35	6.87	6.01	1.61	6.96	64.60	27.72	3.73
0.40	0.16	1.87	324.08	16.68	1.32	6.66	5.84	1.57	6.75	62.24	24.90	4.55
0.45	0.15	1.87	324.56	16.62	1.29	6.44	5.66	1.52	6.54	59.70	22.23	5.42
0.50	**0.15**	**1.87**	**325.17**	**16.57**	**1.25**	**6.21**	**5.47**	**1.48**	**6.31**	**56.95**	**19.71**	**6.34**
0.55	0.14	1.87	326.00	16.51	1.21	5.97	5.28	1.43	6.07	54.00	17.32	7.31
0.60	0.13	1.86	326.94	16.45	1.17	5.71	5.07	1.37	5.81	50.78	15.05	8.32
0.65	0.12	1.85	328.16	16.38	1.12	5.42	4.84	1.31	5.52	47.27	12.92	9.38
0.70	0.12	1.82	329.64	16.32	1.06	5.11	4.58	1.24	5.21	43.38	10.92	10.48
0.75	0.11	1.79	331.47	16.26	1.00	4.76	4.30	1.16	4.86	38.98	9.04	11.63
0.80	**0.09**	**1.73**	**333.78**	**16.20**	**0.91**	**4.34**	**3.95**	**1.06**	**4.44**	**33.88**	**7.30**	**12.82**
0.85	0.08	1.63	336.86	16.15	0.81	3.84	3.53	0.94	3.94	27.46	5.68	14.06
0.90	0.06	1.40	340.28	16.17	0.64	3.16	2.90	0.74	3.23	18.56	4.07	15.29
0.95	0.06	1.03	339.20	16.38	0.53	2.91	2.52	0.62	2.93	11.94	2.62	16.59
1.00	**0.06**	**0.83**	**336.69**	**16.47**	**0.58**	**3.21**	**2.71**	**0.67**	**3.21**	**10.54**	**2.21**	**18.25**

Note: The values in bold represent the points selected to plan the tool wear trials.

Table 10
Pareto-optimal solutions for WS-MMSE approach.

w	Uncoded parameters				Uncoded responses						$f_{(MMSE_1)}$	$f_{(MMSE_2)}$
	F_z	A_p	V_c	A_e	R_a	R_y	R_z	R_q	R_t	MRR		
0.00	0.21	1.70	325.75	17.06	1.55	8.21	7.20	1.88	8.31	76.09	53.87	0.24
0.05	0.21	1.74	324.84	17.02	1.51	8.00	7.00	1.84	8.10	75.04	48.79	0.37
0.10	0.20	1.78	324.05	16.96	1.47	7.74	6.76	1.78	7.83	73.17	42.91	0.85
0.15	0.19	1.82	323.57	16.88	1.43	7.41	6.47	1.71	7.50	70.24	36.42	1.79
0.20	0.17	1.85	323.61	16.77	1.37	7.00	6.12	1.63	7.09	66.05	29.65	3.22
0.25	0.16	1.87	324.39	16.64	1.30	6.51	5.72	1.54	6.61	60.52	23.07	5.14
0.30	0.14	1.87	326.04	16.50	1.21	5.95	5.26	1.42	6.05	53.80	17.17	7.37
0.35	0.12	1.84	328.57	16.37	1.10	5.33	4.77	1.29	5.43	46.15	12.31	9.70
0.40	0.10	1.76	332.00	16.24	0.99	4.68	4.24	1.15	4.78	37.45	8.58	11.93
0.45	0.06	1.20	340.08	16.27	0.55	2.89	2.59	0.64	2.94	14.08	3.24	15.88
0.50	0.05	1.14	339.84	16.31	0.53	2.87	2.54	0.63	2.91	13.21	3.02	16.08
0.55	0.05	1.09	339.60	16.34	0.53	2.88	2.53	0.62	2.91	12.61	2.84	16.27
0.60	0.05	1.05	339.34	16.36	0.53	2.89	2.52	0.62	2.92	12.15	2.69	16.47
0.65	0.06	1.01	339.06	16.38	0.53	2.92	2.53	0.62	2.94	11.79	2.57	16.68
0.70	0.06	0.98	338.77	16.40	0.53	2.95	2.54	0.62	2.97	11.51	2.47	16.89
0.75	0.06	0.95	338.44	16.42	0.54	2.99	2.56	0.63	3.00	11.27	2.38	17.12
0.80	0.06	0.92	338.10	16.43	0.54	3.03	2.59	0.64	3.04	11.07	2.31	17.34
0.85	0.06	0.89	337.75	16.45	0.55	3.07	2.61	0.64	3.08	10.90	2.27	17.57
0.90	0.06	0.87	337.39	16.46	0.56	3.12	2.64	0.65	3.13	10.76	2.23	17.80
0.95	0.06	0.85	337.04	16.46	0.57	3.17	2.67	0.66	3.17	10.64	2.21	18.03
1.00	0.06	0.83	336.69	16.47	0.58	3.21	2.71	0.67	3.21	10.54	2.21	18.25

indicates that, with a reliability of 95%, there is sufficient evidence that not all the means are equal (Johnson and Wichern, 2007). As one can note, the means values of the roughness are significantly different comparing the two approaches. Furthermore, observing the individual CI for individual means, it is immediately clear that the NBI-MMSE approach presents the lowest value for all the roughness responses. The Fisher's method generates grouping information tables for the differences between means. Levels that share a letter are not significantly different (Johnson and Wichern, 2007). It can be seen that no grouping information table is presented for the roughness responses.

Finally, in Table 14, the One-way Manova hypothesis test has emphasized also that the two multivariate approaches studied in this work are statistically different ($p\text{-value} < 0.05$). Manova is used to investigate whether the population mean vectors are the same and, if not, which mean components differ significantly (Johnson and Wichern, 2007).

Taking into account not only the methods' comparative study, but also the detailed analyses among experimental results, it can be concluded that the NBI-MMSE approach has evidenced better properties in relation to another method. The NBI-MMSE presents lower errors between the theoretical values and actual values if compared to the results found for WS-MMSE, indicating application feasibility of such optimization technique multi-objective for correlated responses, applied to the dry end milling of AISI 1045.

With this in mind, Fig. 6(a) and 5(b) show the quality of the machined surface, obtained with the new tool and worn, under the cutting optimal conditions found by the NBI-MMSE approach. The images were taken with a scanning electron microscope (SEM), model Carl Zeiss EVO MA15 (magnification 500×).

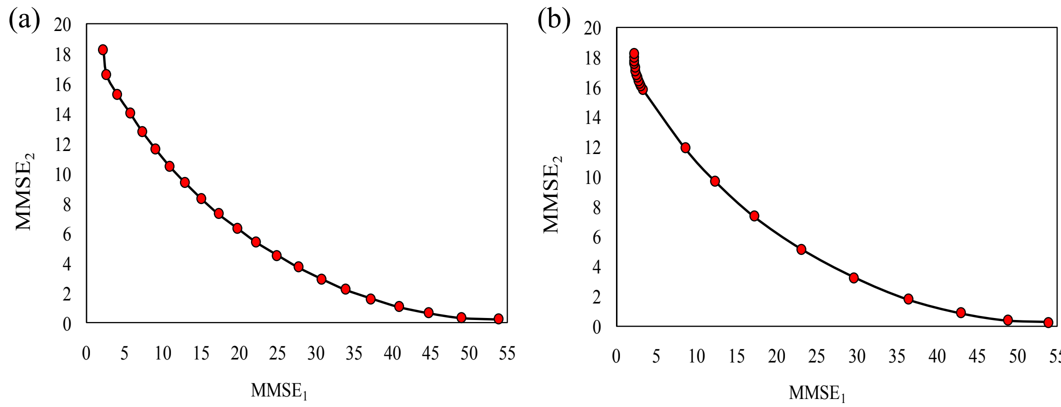

Fig. 5. (a) Pareto Frontier obtained with NBI-MMSE approach (b) WS-MMSE approach.

Table 11
Optimal point for AISI 1045 dry end milling process.

Responses	w	R_a	R_y	R_z	R_q	R_t	MRR
Target values (ζ_{Yi})		0.47	2.71	2.32	0.55	2.72	77.38
Optimal point (NBI-MMSE)	0.8	0.91	4.34	3.95	1.06	4.44	33.88
Optimal point (WS-MMSE)	0.4	0.99	4.68	4.24	1.15	4.78	37.45
Differences of magnitude		0.08	0.34	0.29	0.09	0.34	3.57

Table 14
Manova hypothesis test for the NBI-MMSE and the WS-MMSE approaches.

Criterion	Test statistic	F-test	P-value
Wilk's	0.526	9.009	0.000
Lawley-Hotelling	0.900	9.009	0.000
Pillai's	0.474	9.009	0.000

Table 12
Confirmation test's measurements for NBI-MMSE and WS-MMSE approach.

	Confirmation test (NBI-MMSE)					Confirmation test (WS-MMSE)				
	R_a	R_y	R_z	R_q	R_t	R_a	R_y	R_z	R_q	R_t
Standard-deviation	0.05	0.29	0.15	0.06	0.22	0.09	0.41	0.37	0.10	0.41
Mean	0.95	4.22	3.82	1.09	4.32	1.08	4.48	4.14	1.23	4.60
Prediction value (Optimal point)	0.91	4.34	3.95	1.06	4.44	0.99	4.68	4.24	1.15	4.78
Error (%)	3.75	−2.81	−3.44	2.04	−2.74	8.74	−4.29	−2.41	6.54	−3.95
Lower value (95% CI)	0.77	3.63	3.35	0.91	3.72	0.84	3.98	3.65	1.00	4.08
Higher value (95% CI)	1.06	5.04	4.55	1.22	5.15	1.13	5.37	4.82	1.30	5.47

Note: The percentage error is the difference between mean value and the predicted value.

Table 13
One-Way ANOVA for the means properties of optimization NBI-MMSE and WS-MMSE.

	DF	SS	MS	F-test	P-value	Fisher's method[a]	Diagnostic[a]
Difference between R_a	1	0.24	0.24	44.84	0.000	NBI-MMSE (B)	The R_a mean values of NBI-MMSE (0.95) and
Error	54	0.29	0.01			WS-MMSE (A)	the R_a mean values of WS-MMSE (1.08) are
Total	55	0.52					significant different.
Difference between R_y	1	0.99	0.99	7.84	0.007	NBI-MMSE (B)	The R_y mean values of NBI-MMSE (4.22) and
Error	54	6.85	0.13			WS-MMSE (A)	the R_y mean values of WS-MMSE (4.48) are
Total	55	7.84					significant different.
Difference between R_z	1	1.44	1.44	18.25	0.000	NBI-MMSE (B)	The R_z mean values of NBI-MMSE (3.82) and
Error	54	4.25	0.08			WS-MMSE (A)	the R_z mean values of WS-MMSE (4.14) are
Total	55	5.68					significant different.
Difference between R_q	1	0.28	0.28	38.55	0.000	NBI-MMSE (B)	The R_q mean values of NBI-MMSE (1.09) and
Error	54	0.40	0.01			WS-MMSE (A)	the R_q mean values of WS-MMSE (1.23) are
Total	55	0.68					significant different.
Difference between R_t	1	1.08	1.08	9.76	0.003	NBI-MMSE (B)	The R_t mean values of NBI-MMSE (4.32) and
Error	54	5.98	0.12			WS-MMSE (A)	the R_t mean values of WS-MMSE (4.60) are
Total	55	7.06					significant different.

[a] Considering confidence interval 95.0%.

Besides the surface finishing, tool life (T) is also another important parameter in dry machining. Considering the cutting optimal conditions found by the NBI-MMSE approach (f_z = 0.09 mm/tooth, a_p = 1.73 mm, V_c = 333.78 m/min and a_e = 16.20 mm), tool life trials were measured. For the sake of comparison, tool life trials were also measured in another Pareto-optimal solution. The values in bold shown in Table 9 represent these points (w_0, $w_{0.1}$, $w_{0.5}$, $w_{0.8}$, w_1). These points were chosen to analyze the tool wear under different cutting condition. The T was measured to each cutting pass. Initially, the criteria adopted as the end of tool life was flank wear of approximately $VB_{max} = 0.30$ mm. Fig. 7 presents the growth of principal flank wear (VB) with the numbers of the cutting pass.

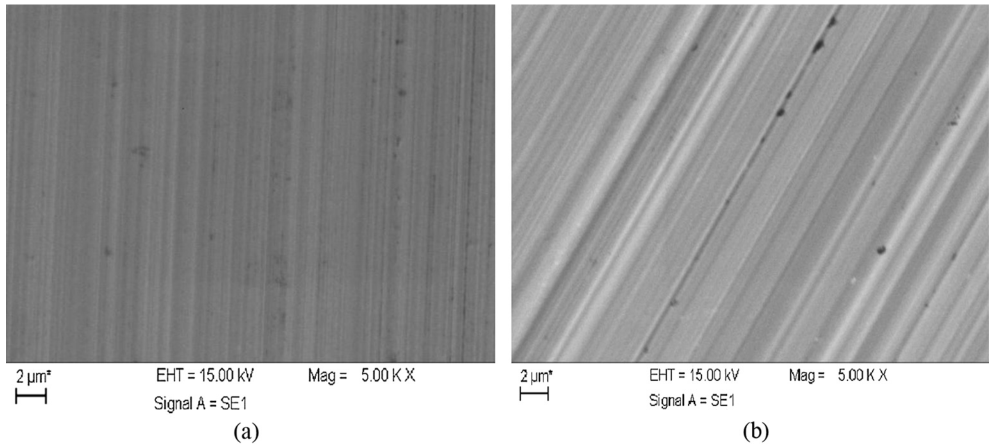

Fig. 6. Machined surface obtained with (a) new tool (b) worn tool (VB = 0.28 mm).

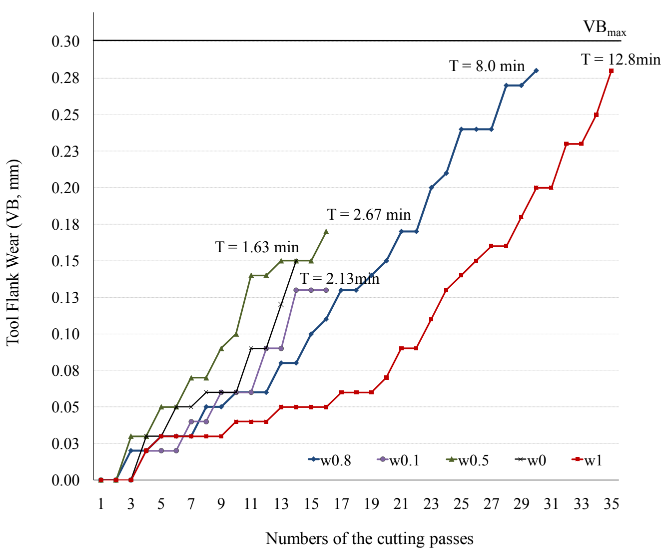

Fig. 7. Tool flank wear VB versus number of the cutting passes.

The results obtained for the end milling process under dry machining have shown that the flank wear rapidly increases with the increases of f_z and a_p. In fact, with w_0, $w_{0.1}$, $w_{0.5}$, the maximum tool life was achieved in 3 min, while with, $w_{0.8}$ and w_1, the maximum tool life was achieved in eight and 12 min, respectively. These results have shown that is possible to use dry machining techniques without affecting the machining process.

Fig. 8 (a) illustrates the tool flank wear (VB) machined on optimal experimental conditions found by NBI-MMSE approach at the tool life end. The tool flank wear was measured with an optical microscope (magnification of 45×) with images acquired by a coupled digital camera. Fig. 8 (b) illustrates the worn tool topography on this same VB. It can be seen that TiCN/TiN coating materials are both removed from the cutting edge to the tool substrate. The images were captured with an SEM (magnification of 500×).

7. Conclusion

This work introduces a mathematical new approach that combine the Normal Boundary Intersection method with Multivariate Mean Square Error functions for optimize multiple correlated responses. This approach combines PCA, the RSM and the concept of MSE. For the sake of comparison, the same procedure was employed to Weighted Sum.

The numerical results indicate that the solution found by NBI-MMSE approach was characterized as a more appropriate optimal point in relation to one obtained with the WS-MMSE. In this case, feed per tooth of 0.09 mm/tooth, axial depth of cut of 1.73 mm,

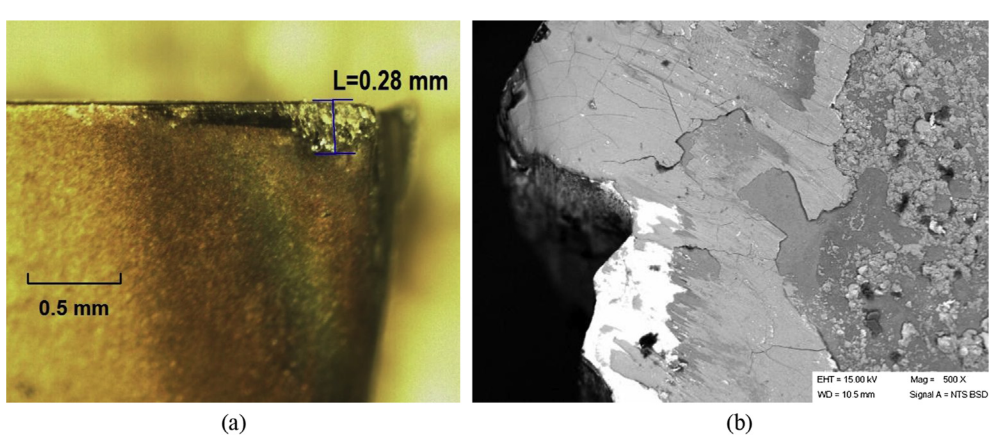

Fig. 8. (a) Tool flank wear (VB = 0.28 mm) (b) Worn tool topography.

ARTICLE IN PRESS

cutting speed of 333.78 m/min, and radial depth of cut of 16.2 mm can be considered as the optimal cutting parameters for minimize roughness and maximize MRR, simultaneously. Furthermore, the tool life trial results obtained by NBI-MMSE approach have shown that is possible to use dry machining techniques without affecting the machining process.

The NBI-MMSE approach outperformed the WS-MMSE as a convex and equispaced frontier, avoiding the agglomeration of Pareto-optimal solutions along the frontier.

The models' capability of predicting the results were verified by the confirmation experiments; low errors were observed between the theoretical and the real values considering a reliability of 95%.

The results presented in this work confirm that, using technical planning for multi-objective optimization, the dry machining techniques can be successfully applied without affecting the machining process results in this case by meaning of surface roughness and material removal rate found.

Acknowledgment

This work was supported by the Brazilian agencies (CNPq, CAPES, FAPEMIG and IFSULDEMINAS).

References

Box, G.E.P., Draper, N.R., 1987. Empirical Model-building and Response Surfaces, first. ed. New Jersey. http://dx.doi.org/10.1037/028110.

Bratchell, N., 1989. Multivariate response surface modeling by principal components analysis. J. Chemom. 3, 579–588. http://dx.doi.org/10.1002/cem.1180030406.

Brito, T.G., Paiva, A.P., Ferreira, J.R., Gomes, J.H.F., Balestrassi, P.P., 2014. A normal boundary intersection approach to multiresponse robust optimization of the surface roughness in end milling process with combined arrays. Precis. Eng. 38, 628–638. http://dx.doi.org/10.1016/j.precisioneng.2014.02.013.

Chahal, M., Sing, V., Garg, R., Kumar, S., 2013. To estimate the range of process parameters for optimization of surface roughness & material removal rate in CNC milling. Int. J. Eng. Trends Technol. (IJETT) 4, 4556–4563.

Das, I., Dennis, J.E., 1998. Normal-Boundary intersection: a new method for generating the pareto surface in nonlinear multicriteria optimization problems. SIAM J. Optim. 8, 631–657. http://dx.doi.org/10.1137/S1052623496307510.

Fratila, D., Caizar, C., 2011. Application of Taguchi method to selection of optimal lubrication and cutting conditions in face milling of AlMg 3. J. Clean. Prod. 19, 640–645. http://dx.doi.org/10.1016/j.jclepro.2010.12.007.

Ginting, A., Nouari, M., 2007. Optimal cutting conditions when dry end milling the aeroengine material Ti – 6242S. J. Mater. Process. Technol. 184, 319–324. http://dx.doi.org/10.1016/j.jmatprotec.2006.10.051.

Jiang, Z., Zhou, F., Zhang, H., Wang, Y., Sutherland, J.W., 2015. Optimization of machining parameters considering minimum cutting fluid consumption. J. Clean. Prod. 108, 183–191. http://dx.doi.org/10.1016/j.jclepro.2015.06.007.

Johnson, R.A., Wichern, D.W., 2007. Applied Multivariate Statistical Analysis, sixth. ed. Pearson Prentice Hall, New Jersey.

Jozić, S., Bajić, D., Celent, L., 2015. Application of compressed cold air cooling: achieving multiple performance characteristics in end milling process. J. Clean. Prod. 100, 325–332. http://dx.doi.org/10.1016/j.jclepro.2015.03.095.

Lin, D.K.J., Tu, W., 1995. Dual response surface optimization. J. Qual. Technol. 27, 34–39.

Montgomery, D.C., 2012. Design and Analysis of Experiments, eighth ed. John Wiley & Sons, Inc., New York, United States of America.

Moshat, S., Datta, S., Bandyopadhyay, A., Pal, P.K., 2010. Parametric optimization of CNC end milling using entropy measurement technique combined with grey-Taguchi method. Int. J. Eng. Sci. Technol. 2, 1–12. http://dx.doi.org/10.4314/ijest.v2i2.59130.

Paiva, A.P., Paiva, E.J., Ferreira, J.R., Balestrassi, P.P., Costa, S.C., 2009. A multivariate mean square error optimization of AISI 52100 hardened steel turning. Int. J. Adv. Manuf. Technol. 43, 631–643. http://dx.doi.org/10.1007/s00170-008-1745-5.

Singh, C., Bhogal, S.S., Pabla, Dr. B.S., Kumar, P., 2014. Empirical modeling of surface roughness and metal removal rate in CNC milling operation. Int. J. Innov. Technol. Res. (JITR) 2, 1120–1126.

Thangarasu, V.S., Devaraj, G., Sivasubramanian, R., 2012. High speed CNC machining of AISI 304 stainless steel; Optimization of process parameters by MOGA. Int. J. Eng. Sci. Technol. 4, 66–77.

Wang, S.-G., Hsu, Y.-L., 2005. One-pass milling machining parameter optimization to achieve mirror surface roughness. Proc. IMechE. Part B J. Eng. Manuf. 219, 177–181. http://dx.doi.org/10.1243/095440505X8064.

Yan, J., Li, L., 2013. Multi-objective optimization of milling parameters e the trade-offs between energy, production rate and cutting quality. J. Clean. Prod. 52, 462–471. http://dx.doi.org/10.1016/j.jclepro.2013.02.030.

Zhang, S., Li, J.F., Wang, Y.W., 2012. Tool life and cutting forces in end milling Inconel 718 under dry and minimum quantity cooling lubrication cutting conditions. J. Clean. Prod. 32, 81–87. http://dx.doi.org/10.1016/j.jclepro.2012.03.014.

Please cite this article in press as: Duarte Costa, D.M., et al., A normal boundary intersection with multivariate mean square error approach for dry end milling process optimization of the AISI 1045 steel, Journal of Cleaner Production (2016), http://dx.doi.org/10.1016/j.jclepro.2016.01.062